IOPscience iopscience.iop.org

Home Search Collections Journals About Contact us My IOPscience

Shallow impurities in multiple V-groove quantum wires

This article has been downloaded from IOPscience. Please scroll down to see the full text article.

2002 J. Phys.: Condens. Matter 14 471

(http://iopscience.iop.org/0953-8984/14/3/315)

View the table of contents for this issue, or go to the journal homepage for more

Download details:
IP Address: 171.66.16.238
The article was downloaded on 17/05/2010 at 04:45

Please note that terms and conditions apply.

INSTITUTE OF PHYSICS PUBLISHING JOURNAL OF PHYSICS: CONDENSED MATTER

J. Phys.: Condens. Matter **14** (2002) 471–482 PII: S0953-8984(02)26949-0

Shallow impurities in multiple V-groove quantum wires

Gerald Weber and Ana M de Paula

Laboratório de Nano-Espectroscopia Óptica, Universidade São Francisco, Av São Francisco de Assis 218, 12916-900 Bragança Paulista SP, Brazil

Received 12 July 2001, in final form 9 October 2001
Published 21 December 2001
Online at stacks.iop.org/JPhysCM/14/471

Abstract

We calculate the binding energies for shallow impurities in multiple V-groove GaAs/AlGaAs quantum wires using a variational technique. The carrier ground states are calculated by an effective potential method together with a suitable coordinate transformation which allows the decoupling of the two-dimensional wavefunction. We present results as a function of impurity position in each wire of multiple quantum wire structures. The dependence of the donor binding energies on the parameters of the wire is discussed. We demonstrate that the interaction between the wires and the symmetry of the impurity wavefunction both have a significant effect on the binding energies in multiple quantum wires.

1. Introduction

The electronic and optical properties of quantum wires have attracted increasing attention recently. Several growth techniques have been successful in obtaining a type of heterostructure known as V-groove or ridge quantum wires. These V-groove structures, single and multiple quantum wires, have been obtained for a variety of II–VI and III–V materials [1–8]. Several optical techniques have revealed properties mainly associated with quantum confined excitonic transitions and also localized excitons from interface monolayer fluctuations [9–19]. Some photoluminescence (PL) spectra also show peaks that have not been clearly identified [9,11,18]. To fully understand the optical and electronic properties of V-groove quantum wires a description of the impurity properties would be important. Impurity-related transitions may be the origin of some of the unknown peaks.

A crucial aspect for theoretical calculations of the physical properties of V-groove quantum wires is to obtain the energy levels and wavefunctions. Several theoretical approaches have been presented: Sa'ar *et al* [20] proposed a local-envelope states expansion, Pescetelli *et al* [21] used a tight-binding approach for T- and V-shaped quantum wires, and Ammann *et al* [22] used a quasi-factorization scheme. However, in general the 2D effective mass Schrödinger equation has been calculated numerically using either plane-wave expansion [23–28] or by adapting finite element methods [29]. Recently we proposed an effective potential method [30]

 © 2002 IOP Publishing Ltd Printed in the UK

which considerably eases the calculation of energy levels and wavefunctions in V-groove quantum wires.

The calculation of shallow impurities in square and circular quantum wires is currently well established [31–34]. However, the variational technique employed for the calculation is numerically intensive if the wire is not circular. Due to the complicated form of the potential profile in V-groove quantum wires the calculation of shallow impurity states may become impractical, or at least restricted to a few impurity positions, if the method of calculation of the carrier ground states is also numerically intensive. Deng *et al* presented calculated donor [35] and acceptor [36] binding energies in single V-groove quantum wires at some specific impurity positions using a coordinate transformation. In a previous paper [37] we reported on the calculation of shallow impurity binding energies in single V-groove quantum wires. We showed that the use of an effective potential method for the calculation of the ground state [30] considerably simplifies the numerical calculation.

For experimental studies of V-groove quantum wires it is important to have a theoretical description of the impurity levels in addition to other physical properties. For instance, for the study of PL spectra it is important to identify the observed peaks as impurity-related or else be able to rule them out as such. The presence of additional structures, such as vertical quantum wells and pinch-off regions, adds new energy states into an already complicated spectrum emphasizing the necessity for a complete level structure calculation. For calculations of impurity-related optical properties, such as impurity absorption coefficients and PL spectra, a detailed knowledge of the impurity binding energy is needed over all spatial regions of the quantum wire. A partial knowledge, for example of a few symmetry points, is not sufficient for this purpose. This calls for a theoretical model which should be numerically very efficient.

In this work we present a calculation of the donor binding energies in multiple V-groove quantum wires using the effective potential method proposed in [30]. The purpose of this paper is to obtain the shallow impurity binding energies and to establish how effectively the shallow impurity responds to the lateral confinement of multiple V-groove quantum wires. We show its numerical efficiency and thus provide an important tool for the study of impurity-related phenomena in multiple V-groove quantum wires.

2. Theory

We first write the Hamiltonian for a Coulombic shallow impurity

$$H = H_0 - \frac{e^2}{4\pi\epsilon[(x - x_{\mathrm{imp}})^2 + (y - y_{\mathrm{imp}})^2 + z^2]^{1/2}} \tag{1}$$

where

$$H_0 = -\frac{\hbar^2}{2m^*}\nabla^2 + V(x, y) \tag{2}$$

is the Hamiltonian without the impurity potential. The impurity position is represented by x_{imp} and y_{imp}, and $V(x, y)$ is the potential profile of the multiple V-groove quantum wire.

We consider multiple quantum wires consisting of N identical quantum wires with well width L_{W} and barrier width L_{B}. The carrier ground state is calculated assuming the following potential profile to describe the interface potentials of the V-groove quantum wire [29, 30]

$$y_1(x) = -b\tan\theta\ln[\cosh(x/b)] + \frac{L_{\mathrm{W}}}{2} \tag{3}$$

$$y_2(x) = y_1(x) - L_{\mathrm{W}} \tag{4}$$

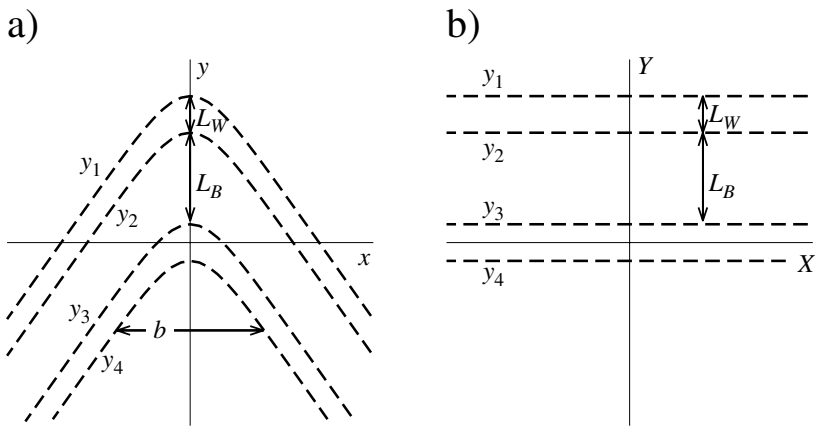

Figure 1. Schematic diagram of the V-shaped interfaces for (*a*) the original coordinates x, y and (*b*) the modified coordinates X, Y.

for the first quantum wire

$$y_3(x) = y_2(x) - L_{\mathrm{B}} \tag{5}$$

$$y_4(x) = y_3(x) - L_{\mathrm{W}} \tag{6}$$

for the second quantum wire, and so on (see figure 1). L_{W} is the channel width along the y direction, L_{B} is the barrier width between the wires and b represents the bend width at the top of the ridge (see figure 1). Here we have defined the angle θ such that $180^\circ - 2\theta$ is the angle between the facets of the ridge, the angle normally referred to in most articles. We then apply the coordinate transformation [29, 30]

$$X = x \qquad Y = -y - b\tan\theta\ln[\cosh(x/b)] \qquad Z = z \tag{7}$$

to the Hamiltonian H_0. In the transformed coordinates the potential barrier becomes linear and resembles that of a multiple quantum well, i.e. it becomes a function of Y only. The transformed Hamiltonian H_0 becomes considerably more complicated as it now contains all the information about the lateral confinement [30]. Our approximation consists of replacing all mixed terms of the transformed Hamiltonian by an effective lateral potential [30]

$$V_{\mathrm{eff}}(X) = V_X \tan\theta \tanh^2(X/b) \tag{8}$$

where V_X is an angle-independent barrier factor. This potential allows the decoupling of the the two-dimensional Hamiltonian into two one-dimensional Hamiltonians

$$-\frac{\hbar^2}{2m^*}\frac{\mathrm{d}^2 f(X)}{\mathrm{d}X^2} + U(X)f(X) = E_x f(X) \tag{9}$$

$$-\frac{\hbar^2}{2m^*}\frac{\mathrm{d}^2 g(Y)}{\mathrm{d}Y^2} + W(Y)g(Y) \ = E_y g(Y) \tag{10}$$

with the wavefunctions given by $\phi(X, Y) = f(X)g(Y)$ and the total energy by $E = E_x + E_y$. The two-dimensional potential is given by $V(X, Y) = U(X) + W(Y)$. The Schrödinger equation in the X-direction, equation (9), now contains only the $U(X)$ potential, equation (8), which we solve by the Numerov method [38]. In the Y-direction the potential $W(y)$ represents a multiple quantum well; equation (10) can be solved by usual transfer matrix techniques [39–42]. For more a detailed discussion about this method please see [30].

The impurity binding energy is calculated using a standard variational technique; for details see [31,43,44]. The trial wavefunction is chosen as

$$\psi(X, Y, Z) = N\phi(X, Y) \exp\left\{ -\left[(X - X_{\text{imp}})^2 + (Y - Y_{\text{imp}})^2 + Z^2\right]^{1/2} / \lambda \right\} \tag{11}$$

where X_{imp}, Y_{imp} is the impurity position in transformed coordinates and λ is the variational parameter. $\phi(X, Y)$ is the ground state wavefunction without the impurity, i.e. the eigenfunction of H_0 obtained in transformed coordinates. All calculations are carried out in transformed coordinates. The binding energy $E_{\text{B}} = E_0 - E$ is obtained by numerically minimizing the energy E with respect to the variational parameter λ, where E_0 is the ground energy level without the impurity. In the appendix we outline some important simplifications that reduce the numerical computation considerably. To the best of our knowledge, these simplifications have not yet been presented elsewhere.

3. Results and discussion

We present results for GaAs/$Al_{0.3}Ga_{0.7}$As V-groove quantum wires and we discuss the binding energies for donor impurities as a function of impurity position in the wire. We used the effective masses for GaAs of $0.067m_0$ and a dielectric constant of $13.18\epsilon_0$ [45]. The effective Bohr radius for these parameters is $a_0 = 9.75$ nm. The barrier height is 264 meV for the conduction band [29]. Also, we use a barrier factor V_X of 42.4 meV for the conduction band [30]. The angle is $\theta = 54.75^\circ$ such that $180^\circ - 2\theta$ corresponds to the measured angle between the two facets of the ridge [29,30]. For comparison we also consider a smaller angle (larger angle between the facets) of $\theta = 30^\circ$, since we notice that for multiple V-groove quantum wires the angle between the facets ($180^\circ - 2\theta$) becomes increasingly larger (e.g. [7]). In this section we will refer to the wires shown in the figures as first, second and third counting from top to bottom.

The donor binding energies as a function of the impurity position x_{imp} and y_{imp} are presented in figure 2 for double V-groove quantum wires with a channel width of 4 nm and bend width of 4 nm. The barrier width between the two wires is also 4 nm. The contour plots show curves with the same impurity binding energy, which is incremented by 1 meV for each curve towards the centre of the wire. For the first (upper) quantum wire the binding energies are larger, 16.4 meV at the centre, than for the second (lower) wire, 15.5 meV. Both are smaller than the binding energy of 23 meV for a single quantum wire with the same width [37]. This is an effect of delocalization of the impurity wavefunction due to the presence of a second wire. Figure 3 shows the impurity wavefunctions at the centre of each quantum wire. The wavefunction for a donor located at the centre of the first wire can now penetrate into the second wire. However, the wavefunction of donor located at the centre of the second wire is even less confined (and therefore has a lower binding energy) and penetrates quite considerably into the first wire. This asymmetry results from the lateral confinement due to the bend in the wire.

For a triple quantum wire structure, shown in figure 4, the largest binding energy is 15.8 meV at the second wire. This is smaller than the largest binding energy for double quantum wires with the same widths. The first and third wire present smaller binding energies, 12.9 and 11.9 meV, respectively. Now the second wire has the most symmetric wavefunction (see figure 5(*b*)) and thus a stronger impurity localization. The binding energies depend mainly on two factors regarding the wavefunction: confinement due to the barrier and its symmetry. For quantum wire structures with larger wires these effects are much less pronounced, as shown in figure 6, since there is less interaction between the wires. Again, the largest binding energy is for the second wire (15.8 meV), while the first and third wires have smaller binding energies (14.4 and 12.6 meV respectively). Note that the binding energies are more similar for each wire,

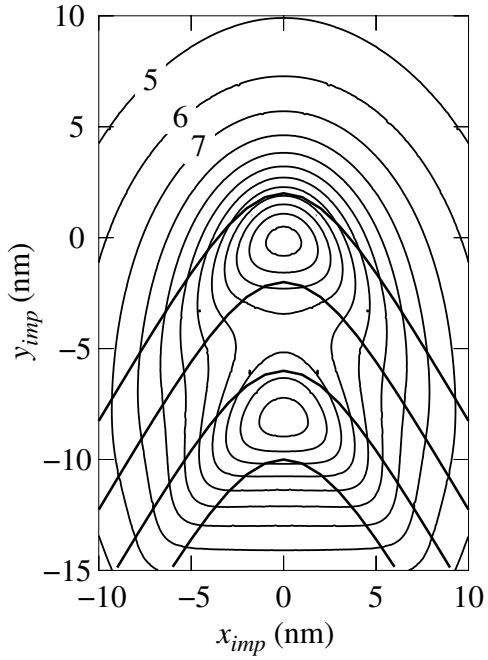

Figure 2. Calculated donor binding energies as a function of the impurity position $x_{\rm imp}$ and $y_{\rm imp}$ for a double quantum wire structure. The contour plots show curves with the same binding energy listed in meV (for some curves), the energy increments by 1 meV for each curve towards the centre of the wire. The dimensions of the V-groove quantum wire are $b = L_{\rm W} = L_{\rm B} = 4$ nm and angle $\theta = 54.75^{\circ}$.

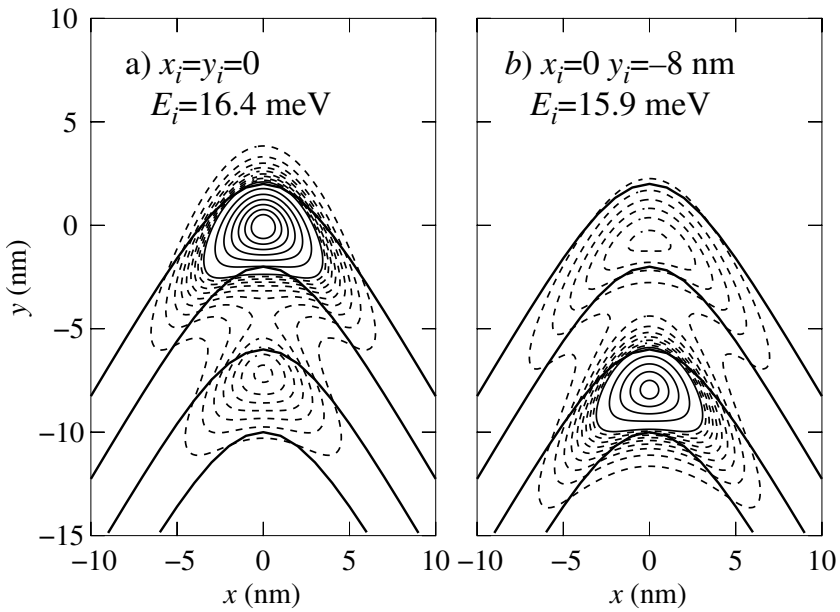

Figure 3. Contour plots for $|\psi(x, y, 0)|^2$ for a donor located at (*a*) $x_{\rm imp} = y_{\rm imp} = 0$ and (*b*) $x_{\rm imp} = 0$, $y_{\rm imp} = -8$ nm for the same structure as shown in figure 2. The outermost dashed curve is for 0.2 a_0^{-3}, with increments of 0.2 a_0^{-3} between each dashed curve. For full curves, the outermost is 2 a_0^{-3}, with increments of 1 a_0^{-3}.

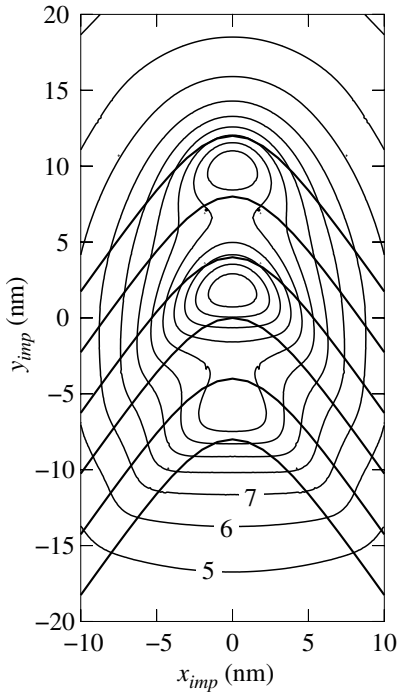

Figure 4. Calculated donor binding energies as a function of the impurity position x_{imp} and y_{imp} for a triple quantum wire structure. The contour plots show curves with the same binding energy listed in meV (for some curves), the energy increments by 1 meV for each curve towards the centre of the wire. The dimensions of the V-groove quantum wire are $b = L_{\mathrm{W}} = L_{\mathrm{B}} = 4$ nm and angle $\theta = 54.75^{\circ}$.

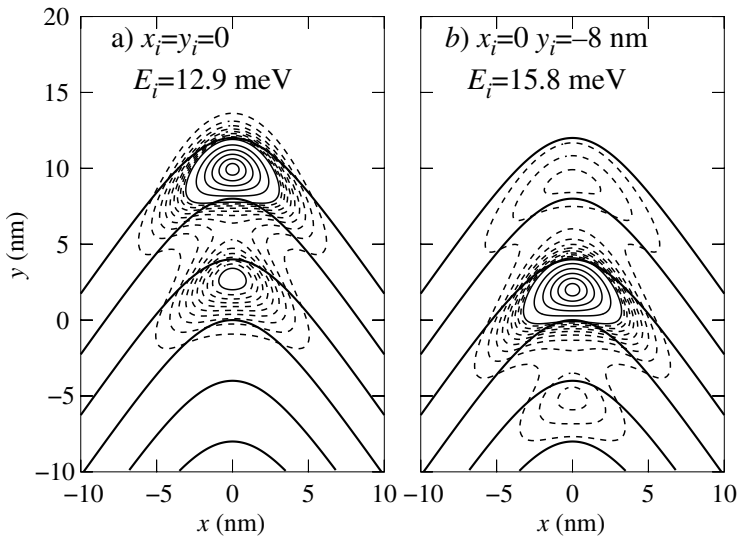

Figure 5. Contour plots for $|\psi(x, y, 0)|^2$ for a donor located at (*a*) $x_{\mathrm{imp}} = y_{\mathrm{imp}} = 0$ and (*b*) $x_{\mathrm{imp}} = 0$, $y_{\mathrm{imp}} = -8$ nm for the same structure as shown in figure 4. The outermost dashed curve is for 0.2 a_0^{-3}, with increments of 0.2 a_0^{-3} between each dashed curve. For full curves, the outermost is 2 a_0^{-3}, with increments of 1 a_0^{-3}.

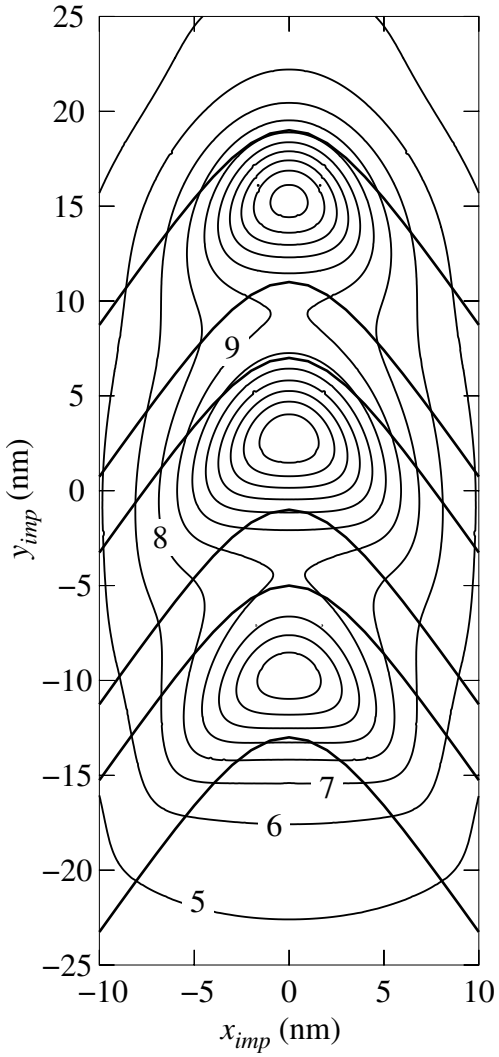

Figure 6. Calculated donor binding energies as a function of the impurity position $x_{\rm imp}$ and $y_{\rm imp}$ for a triple quantum wire structure. The contour plots show curves with the same binding energy listed in meV (for some curves), the energy increments by 1 meV for each curve towards the centre of the wire. The dimensions of the V-groove quantum wire are $b = L_{\rm B} = 4$ nm, $L_{\rm W} = 8$ nm and angle $\theta = 54.75^{\circ}$.

which is to be expected as there is less interaction between the wires. Also, they are all smaller when compared with the thinner wire structure as there is less confinement. Figure 7 shows the results for a triple quantum wire structure with a smaller angle θ. The largest binding energy is also at the centre of the second wire. The binding energies are all smaller than those for the previous structures due to a weaker lateral confinement. They are also more similar for each wire.

Figure 8 shows the variation of the on-centre binding energies as a function of structure parameters: well width, barrier width and bending angle. The dependence on the effective potential parameter V_X (barrier factor) is also shown in figure 8(d). Note that it takes a considerable variation in the barrier factor to significantly change the binding energies. Therefore, the binding energies are not sensitive to small variations in the barrier factor V_X.

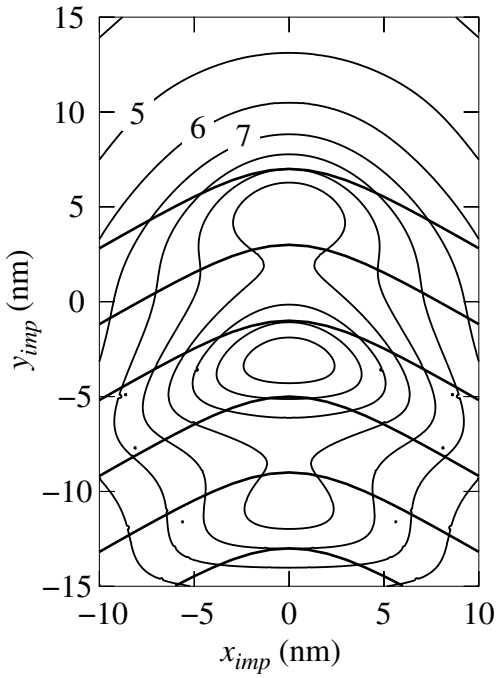

Figure 7. Calculated donor binding energies as a function of the impurity position x_{imp} and y_{imp} for a triple quantum wire structure. The contour plots show curves with the same binding energy listed in meV (for some curves), the energy increments by 1 meV for each curve towards the centre of the wire. The dimensions of the V-groove quantum wire are $b = L_{\mathrm{W}} = L_{\mathrm{B}} = 4$ nm and angle $\theta = 30^{\circ}$.

It can be noted that the donor binding energy depends on the details of the structure in a non-trivial way. The confinement, the interaction between the wires and also the structure symmetry are important determinants of the donor properties. In general, a more confined and more symmetric impurity wavefunction results in larger binding energies.

The results for double and triple quantum wire structures already show the main features of the binding energies in multiple quantum wire structures. However, there is no limit or constraint to calculating the binding energies for structures with an arbitrary number of quantum wires. Due to the complete decoupling of wavefunctions the computational cost of calculating the impurity binding energy is independent of the number of wires. For structures with a large number of quantum wires, the binding energies become smaller overall, as shown in figure 9 for a multiple quantum wire structure with 10 quantum wires. Also, the asymmetry effects are less visible for such large structures. Nonetheless, the overall physical properties are much the same as for the double and triple quantum wires.

4. Conclusion

We have studied the shallow donor properties in multiple V-groove quantum wires. The binding energies are calculated by an effective potential method. We show results as a function of impurity position in each wire of multiple quantum wires and we demonstrate that the dependence of the donor binding energies on the structure parameters is non-trivial. In multiple quantum wire structures the interaction between the wires and the symmetry of the impurity wavefunction have a significant effect on the binding energies.

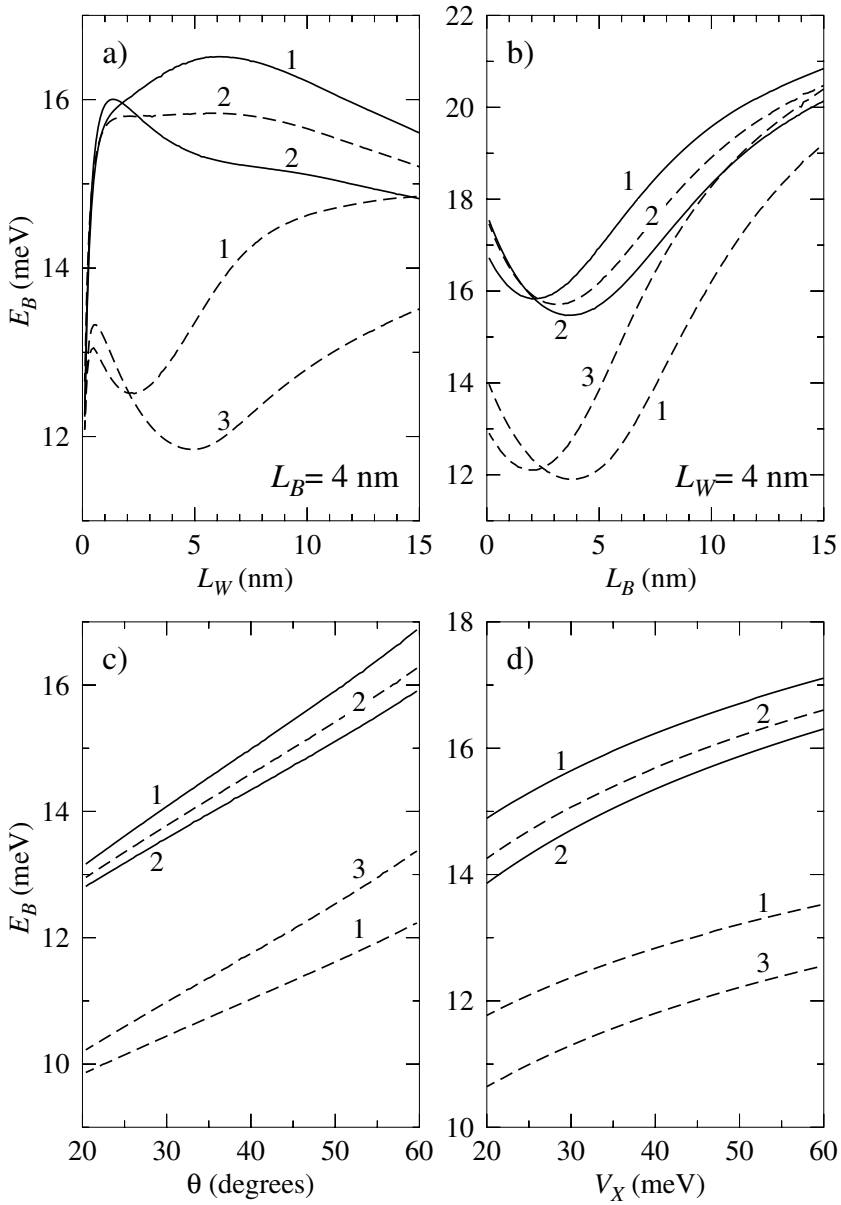

Figure 8. Calculated donor binding energies as a function of (*a*) well width, (*b*) barrier width, (*c*) bending angle and (*d*) barrier factor. Full (dashed) curves are for a double (triple) quantum wire structures. The numbers for each curve indicate the wire where binding energies were calculated. The actual impurity position is for the centre of its corresponding wire. Structure parameters are $L_{\mathrm{W}} = 4$ nm, $L_{\mathrm{B}} = 4$ nm, $\theta = 54.75^{\circ}$ and $V_X = 42.4$ meV unless indicated otherwise.

Acknowledgments

We acknowledge financial support from CNPq (522789/96-0, 300917/91-0) and Fapesp (96/10871-1).

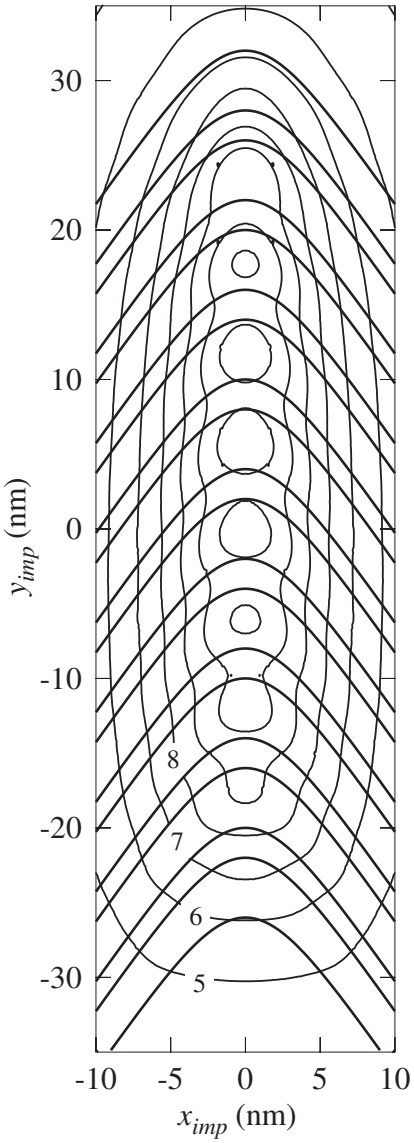

Figure 9. Calculated donor binding energies as a function of the impurity position x_{imp} and y_{imp} for a quantum wire structure with 10 wires. The contour plots show curves with the same binding energy listed in meV (for some curves), the energy increments by 1 meV for each curve towards the centre of the wire. The dimensions of the V-groove quantum wire are $b = L_{\mathrm{W}}4$ nm, $L_{\mathrm{B}} = 2$ nm and angle $\theta = 54.75^{\circ}$.

Appendix. Simplification of the kinetic energy and confinement terms

The expectation energy $E = \langle\psi|H|\psi\rangle$ can be separated into three terms. The kinetic energy term

$$K = \langle\psi| - \frac{\hbar^2}{2m^*}\nabla^2|\psi\rangle \tag{A.1}$$

the term due to the two-dimensional confining potential

$$C = \langle\psi|V(x, y)|\psi\rangle \tag{A.2}$$

and the impurity potential term

$$I = \langle\psi| - \frac{e^2}{4\pi\epsilon r}|\psi\rangle \tag{A.3}$$

with $r = [(x - x_i)^2 + (y - y_i)^2 + z^2]^{1/2}$, such that $E = K + C + I$.

We assume that ψ can be written in the following form

$$\psi = \phi(x, y)\mathrm{e}^{-r/\lambda} \qquad \phi(x, y) = g(x)f(y) \tag{A.4}$$

where ϕ is the ground state without the impurity. Also, we assume that the potential $V(x, y)$ can be written as

$$V(x, y) = U(x) + W(y). \tag{A.5}$$

Then it is straightforward to show that the kinetic energy term becomes

$$K = \frac{\hbar^2}{2m^*\lambda^2} + E_x + E_y - C \tag{A.6}$$

where E_x and E_y are the eigenenergies without the impurity in the x and y directions respectively. This result is obtained by replacing the second-order derivatives of $g(x)$ and $f(x)$ by

$$\frac{\partial^2 g(x)}{\partial x^2} = \frac{2m^*}{\hbar^2}[U(x) - E_x]\,g(x) \tag{A.7}$$

$$\frac{\partial^2 f(y)}{\partial y^2} = \frac{2m^*}{\hbar^2}\left[W(y) - E_y\right]f(y) \tag{A.8}$$

in the kinetic energy term.

The expectation energy becomes simply

$$E = \frac{\hbar^2}{2m^*\lambda^2} + E_x + E_y + I \tag{A.9}$$

since the term corresponding to the confining potential in equation (A.2) is cancelled. The problem is thus reduced to numerically calculating the impurity potential term I in equation (A.3).

References

[1] Cingolani R, Sogawa F, Arakawa Y, Rinaldi R, DeVittorio M, Passaseo A, Taurino A, Catalano M and Vasanelli L 1998 *Phys. Rev.* B **58** 1962

[2] Martinet E, Reinhardt F, Gustafsson A, Biasol G and Kapon E 1998 *Appl. Phys. Lett.* **72** 701

[3] Kappelt M, Grundmann M, Krost A, Türck V and Bimberg D 1996 *Appl. Phys. Lett.* **68** 3596

[4] Türck V, Stier O, Heinrichsdorff F, Grundmann M and Bimberg D 1995 *Appl. Phys. Lett.* **67** 1712

[5] Gustafsson A, Reinhardt F, Biasiol G and Kapon E 1995 *Appl. Phys. Lett.* **95** 3673

[6] Wang X L, Ogura M and Matsuhata H 1995 *Appl. Phys. Lett.* **66** 1506

[7] Biasiol G, Kapon E, Ducommun Y and Gustafson A 1998 *Phys. Rev.* B **57** R9416

[8] Gurevich S A *et al* 1998 *Semicond. Sci. Technol.* **13** 139

[9] Wang X L, Ogura M, Matsuhata H and Tada T 1997 *Superlatt. Microstruct.* **22** 221

[10] Ben-Ami U *et al* 1998 *Appl. Phys. Lett.* **73** 1619

[11] Tribe W R, Steer M J, Forshaw A N, Schumacher K L, Mowbray D J, Whittaker D M, Skolnick M S, Roberts J S and Hill G 1998 *Appl. Phys. Lett.* **98** 3420

[12] Emiliani V, Lienau C, Hauert M, Colí G, DeGiorgi M, Rinaldi R, Passaseo A and Cingolani R 1999 *Phys. Rev.* B **60** 13 335

[13] Lomascolo M, Rinaldi R, Passaseo A, Vittorio M D, Giorgi M D, Cingolani R, Caro L D, Tapfer L, Taurino A and Catalano M 1999 *J. Phys.: Condens. Matter* **11** 5989
[14] Lomascolo M, Giorgi M D, Anni M, Rinaldi R, Passaseo A, Taurino M D V A, Catalano M, Lorenzoni A, Andreani L C and Cingolani R 2000 *Physica* E **7** 536
[15] Achermann M, Nechay B A, Siegner U, Hartmann A, Oberli D, Kapon E and Keller U 2000 *Appl. Phys. Lett.* **76** 2695
[16] Martinet E, Dupertuis M A, irigu L, Oberli D Y, Rudra A, Leifer K and Kapon E 2000 *Phys. Status Solidi* a **178** 233
[17] Oberli D Y, Vouilloz F, Ambigapathy R, Deveaud B and Kapon E 2000 *Phys. Status Solidi* a **178** 211
[18] Liu X Q, Sasaki A, Ohno N, Wang X L and Ogura M 2000 *Appl. Phys. Lett.* **77** 1481
[19] Crottini A, Staehli J L, Deveaud B, Wang X L and Ogura M 2001 *Phys. Rev.* B **63** 121313
[20] Sa'ar A, Calderon S, Givant A, Ben-Shalom O, Kapon E and Caneau C 1996 *Phys. Rev.* B **54** 2675
[21] Pescetelli S, Di Carlo A and Lugli P 1997 *Phys. Rev.* B **56** R1668
[22] Ammann C, Dupertius M A, Bockelmann U and Deveaud B 1997 *Phys. Rev.* B **55** 2420
[23] Rinaldi R *et al* 1994 *Phys. Rev. Lett.* **73** 2899
[24] Kiener C, Rota L, Freyland J M, Turner K, Maciel A C, Ryan J F, Marti U, Martin D, Morier-Gemoud F and Reinhart F K 1995 *Appl. Phys. Lett.* **67** 2851
[25] Rinaldi R, Giugno P V, Cingolani R, Rossi F, Molinari E, Marti U and Reinhart F K 1996 *Phys. Rev.* B **53** 13 710
[26] Ryan J F, Maciel A C, Kiener C, Rota L, Turner K, Freyland J M, Marti U, Martin D, Morier-Gemoud F and Reinhart F K 1996 *Phys. Rev.* B **53** R4225
[27] Chang K and Xia J B 1998 *Phys. Rev.* B **58** 2031
[28] Fu Y, Willander M, Liu X Q, Lu W, Shen S C, Tan H H, Jagadish C, Zou J and Cockayne D J H 2001 *J. Appl. Phys.* **89** 2351
[29] Inoshita T and Sakaki H 1996 *J. Appl. Phys.* **79** 269
[30] Creci G and Weber G 1999 *Semicond. Sci. Technol.* **14** 690
[31] Weber G, Schulz P A and Oliveira L E 1988 *Phys. Rev.* B **38** 2179
[32] Latgé A and Oliveira L E 1995 *J. Appl. Phys.* **77** 1328
[33] Latgé A, de Dios-Leyva M and Oliveira L E 1994 *Phys. Rev.* B **49** 10 450
[34] Villamil P, Porras-Montenegro N and Granada J C 1999 *Phys. Rev.* B **59** 1605
[35] Deng Z Y, Chen X, Ohji T and Kobayashi T 2000 *Phys. Rev.* B **61** 15 905
[36] Deng Z Y, Chen X and Ohji T 2000 *J. Phys.: Condens. Matter* **12** 3019
[37] Weber G and de Paula A M 2001 *Phys. Rev.* B **63** 113307
[38] Quiroz González J L M and Thompson D 1997 *Comput. Phys.* **11** 514
[39] Yang Z, Weiss B L and Li E H 1995 *Superlatt. Microstruct.* **17** 177
[40] Deck R T and Li X 1995 *Am. J. Phys.* **63** 920
[41] Sugg A R and Leburton J P C 1990 *IEEE J. Quantum Electron.* **27** 224
[42] Chang Y C 1982 *J. Vac. Sci. Technol.* **21** 540
[43] Weber G, Schulz P A and Oliveira L E 1989 *Mater. Sci. Forum* **38–41** 1415
[44] Weber G and Oliveira L E 1990 *Mater. Sci. Forum* **65–66** 135
[45] Adachi S 1985 *J. Appl. Phys.* **58** R1